X-ray Crystallographic Structures of D-Xylose Isomerase–Substrate Complexes Position the Substrate and Provide Evidence for Metal Movement during Catalysis[†,‡]

Arnon Lavie, Karen N. Allen, Gregory A. Petsko, and Dagmar Ringe*

Departments of Biochemistry and Chemistry and Rosenstiel Basic Medical Sciences Research Center, Brandeis University, 415 South Street, Waltham, Massachusetts 02254-9110

Received January 13, 1994; Revised Manuscript Received March 2, 1994[⊕]

ABSTRACT: The X-ray crystallographic structures of the metal-activated enzyme xylose isomerase from *Streptomyces olivochromogenes* with the substrates D-glucose, 3-*O*-methyl-D-glucose and in the absence of substrate were determined to 1.96-, 2.19-, and 1.81-Å resolution and refined to *R*-factors of 16.6%, 15.9%, and 16.1%, respectively. Xylose isomerase catalyzes the interconversion between glucose and fructose (xylose and xylulose under physiological conditions) by utilizing two metal cofactors to promote a hydride shift; the metals are bridged by a glutamate residue. This puts xylose isomerase in the small but rapidly growing family of enzymes with a bridged bimetallic active site, in which both metals are involved in the chemical transformation. The substrate 3-*O*-methylglucose was chosen in order to position the glucose molecule in the observed electron density unambiguously. Of the two essential magnesium ions per active site, Mg-2 was observed to occupy two alternate positions, separated by 1.8 Å, in the substrate-soaked structures. The deduced movement was not observed in the structure without substrate present and is attributed to a step following substrate binding but prior to isomerization. The substrates glucose and 3-*O*-methylglucose are observed in their linear extended forms and make identical interactions with the enzyme by forming ligands to Mg-1 through O2 and O4 and by forming hydrogen bonds with His53 through O5 and Lys182 through O1. Mg-2 has a water ligand that is interpreted in the crystal structure in the absence of substrate as a hydroxide ion and in the presence of substrate as a water molecule. This hydroxide ion may act as a base to deprotonate the glucose O2 and subsequently protonate the product fructose O1 concomitant with hydride transfer. Calculations of the solvent-accessible surface of possible dimers, with and without the α-helical C-terminal domain, suggest that the tetramer is the active form of this xylose isomerase.

D-Xylose isomerase (EC 5.3.1.5) is an extensively utilized enzyme in industry in the production of high-fructose corn syrup, due to its ability to isomerize D-glucose into D-fructose. The physiological substrate is probably D-xylose, which is converted into D-xylulose. The mechanistic interest in xylose isomerase originates from the fact that it appears to catalyze an isomerization reaction, not by the well-studied proton-transfer mechanism but by a hydride shift promoted by a bridged bimetallic center.

Xylose isomerase had been assumed to function in a fashion analogous to triosephosphate isomerase (TIM); both enzymes catalyze similar chemical reactions (isomerization of D-glyceraldehyde 3-phosphate to dihydroxyacetone phosphate by TIM and xylose to xylulose by xylose isomerase) and both belong to the α/β-barrel structural family of proteins (Reider & Rose, 1959; Albery & Knowles, 1976; Farber & Petsko, 1990). However, while the rate of isomerization by TIM is diffusion-controlled (Blacklow et al., 1988), the turnover rate of xylose isomerase is 5 orders of magnitude slower. This difference in rate has been attributed to mechanistic differences: TIM proceeds by general acid–base catalysis through an enediol intermediate whose formation and breakdown is catalyzed by active-site residues; in contrast, the isomerization reaction catalyzed by xylose isomerase is dependent on the chemistry of metal cofactors, two of which are bound per active site (Allen et al., 1994a). A further difference between the two enzymes is that xylose isomerase catalyzes ring opening of the substrate prior to isomerization (Allen et al., 1994b).

The X-ray crystal structures of xylose isomerases from different bacterial strains have been solved and were found to be very similar: *Actinoplanes missouriensis* (Rey et al., 1988; Jenkins et al., 1992), *Arthrobacter* (Henrick et al., 1989; Collyer et al., 1990), *Streptomyces rubiginosus* (Carrell et al., 1984; Whitlow et al., 1991), *Clostridium thermosulfurogenes* (Meng et al., 1991), *Streptomyces albus* (Dauter et al., 1990), and *Streptomyces olivochromogenes* (Farber et al., 1987). Determination of precise substrate orientation with relation to the metals and the other active-site residues is important to an understanding of the mechanism of this enzyme. To this end, several structures of xylose isomerase with substrates present (Collyer et al., 1990; Whitlow et al., 1991; Jenkins et al., 1992) or with inhibitors bound (Henrick et al., 1989; Collyer et al., 1990, 1992; Collyer & Blow, 1990; Whitlow et al., 1991; Jenkins et al., 1992) have been solved. However, there is an intrinsic difficulty in the interpretation of the resulting electron density maps. This difficulty arises because xylose isomerase binds its substrates weakly (as can be inferred from the high K_M values for substrates, 5 and 290 mM for xylose and glucose, respectively; Lambeir et al., 1992), resulting in low occupancy of the substrate in the active site. Attempts to compensate for the low binding affinity by

[†] This work was supported by National Institutes of Health Grants GM26788 and GM32410 (to D.R. and G.P.), by American Cancer Society Fellowship PF3560 (to K.N.A.), and in part by a grant from the Lucille P. Markey Charitable Trust.

[‡] The coordinates of the structures have been deposited in the Brookhaven Protein Data Bank under the code names 1XYA, 1XYB, and 1XYC.

* Author to whom correspondence should be addressed.

[⊕] Abstract published in *Advance ACS Abstracts*, April 15, 1994.

0006-2960/94/0433-5469$04.50/0 © 1994 American Chemical Society

increasing the substrate concentration can result in nonproductive binding. Moreover, the linear forms of glucose or xylose lack a recognizable feature to aid in their fitting into an electron density map.

To establish the orientation of the sugar unambiguously, the glucose analog 3-*O*-methyl-D-glucose was used. This compound was chosen as it fulfills a number of important criteria: it is a substrate of xylose isomerase with a K_M similar to that of glucose; it is stereochemically similar to glucose so that it can be expected to bind in a manner similar to glucose, yet the methylated 3-position can act as a guide in the placement of the compound into the electron density. Therefore, xylose isomerase crystals were soaked with D-glucose and with 3-*O*-methyl-D-glucose, and X-ray data were collected. Unambiguous interpretation of the substrate orientation was possible by comparing the resulting electron densities and noting the extra density for the methyl group at the 3-position. At the same time, we have extended the resolution for the unbound *S. olivochromogenes* xylose isomerase structure to 1.8 Å for purposes of comparison. On the basis of these results and observations made by ourselves and others concerning xylose isomerase, we propose a detailed mechanism for isomerization.

MATERIALS AND METHODS

Materials. D-Xylose isomerase (EC 5.3.1.5) from *Streptomyces olivochromogenes* was prepared as described earlier (Allen et al., 1994b). The substrate α-D-glucose was purchased from Sigma Chemical Company. 3-*O*-methyl-D-glucose was purchased from Aldrich Chemical Company. Both were used without further purification.

Crystallization and Data Collection. Crystallization conditions for xylose isomerase were reported previously (Farber et al., 1987). Crystals were soaked with the appropriate substrates at concentrations of 600 mM in 25 mM Hepes buffer and (pH 7.4) 60% saturated $(NH_4)_2SO_4$ for at least 24 h; all buffers contained 10 mM $MgCl_2$. Three data sets were collected: native, native plus glucose, and native plus 3-*O*-methylglucose. The native xylose isomerase data set was collected at Brandeis University on a Rigaku R-Axis image plate detector system mounted on a Rigaku RU200 X-ray generator using a copper anode. The data were reduced using the Rigaku IIc software package supplied by Molecular Structure Corporation. The glucose data set was kindly collected by Dr. Emil F. Pai at the Max Planck Institute (Heidelberg, FRG), using a Siemens multiwire detector mounted on an Elliot GX-13 X-ray generator. Data were reduced by the program XDS (Kabsch, 1988). The 3-*O*-methylglucose data set was collected at the EMBL in Hamburg, FRG, using an MAR Research image plate detector system. The X-ray source was a sealed tube generator with a molybdenum target. Data reduction was performed using the DENZO software package (Z. Otwinowski, Yale University).

Molecular Replacement. The structure of *S. olivochromogenes* xylose isomerase has been solved previously at 3-Å resolution in the pseudo-space group *I*222 by the method of multiple isomorphous replacement (Farber et al., 1987). The structure in the true primitive space group of the crystals was determined by the molecular replacement method. Molecular replacement was performed first in the pseudosymmetric space group *I*222 using a monomer as the asymmetric unit. The starting model was one subunit of the higher resolution refined structure of *Arthrobacter* xylose isomerase (Brookhaven Protein Data Bank entry PDB4XIA.ENT; Collyer et al., 1990), with the sorbitols, magnesiums, and waters deleted. Molecular replacement calculations used a variant of the Rossmann and Blow (1962) rotation function with the Lattman Θ_+,Θ_- coordinate system. Rotation function space group 4 (Rao et al., 1980), which has eight equivalent positions (symbol $Pbc2_1$), was used to find the unique solution. The translation function used was that of Crowther and Blow (1967). Again, a unique solution was found. Finally, the monomer model from *Arthrobacter* was rotated and translated using these solutions, and the sequence was changed using FRODO (Jones, 1978) into the sequence of *S. olivochromogenes* xylose isomerase. The initial position of the dimer in the asymmetric unit was then generated from this monomer by applying the transformation matrix between the pseudo-space group *I*222 and the true space group $P2_12_12$.

Refinement. All models were subjected to refinement by XPLOR (Brünger, 1992), with manual rebuilding performed between refinement cycles on an Evans & Sutherland graphics station running FRODO (Jones, 1978). The first structure refined was that of the 3-*O*-methylglucose complex, which gave an *R*-factor of 26.4% after one cycle of XPLOR using the coordinates from the molecular replacement. The substrate was not included in the initial model to avoid phase bias. Waters were added using the program Waterhunter (S. Sugio, unpublished results), refined, and checked individually for their fit into difference electron density maps calculated with coefficients $3F_{obs} - 2F_{calc}$ using a 1σ cutoff. When the *R*-factor was 18.2%, the difference Fourier map with coefficients $F_{obs} - F_{calc}$ clearly showed how to fit the 3-*O*-methylglucose into the density. Further refinement cycles were performed with the sugar present in the model. The native structure and the glucose complex structure were refined in a similar manner using the above partially refined 3-*O*-methylglucose complex structure, omitting the sugars and the waters. In all structures, the last cycle consisted of a simulated annealing omit map (Hodel et al., 1992) where the substrates and ligand side chains were omitted from the models. The electron density maps produced confirmed the positions of the ligands, metals, and substrates.

Analytical Procedures. Activity and protein assays were performed as previously described (Allen et al., 1994b). The kinetic parameters of 3-*O*-methylglucose were compared to those of glucose using the same assay procedure as was used for glucose.

RESULTS

Refinement Statistics. All three data sets, although collected on three different machines and processed by three different software packages, showed a high level of agreement when comparing F_{obs} (largest difference was 11.5%) and resulted in very small Cα rms differences for the final refined structures (largest overall rms difference 0.2 Å). Data collection and refinement statistics are shown in Table 1.

Overall Structure. Xylose isomerase crystallizes in space group $P2_12_12$, with unit cell dimensions $a = 87.7$ Å, $b = 99.4$ Å, $c = 94.3$ Å and with a dimer in the asymmetric unit. However, the diffraction pattern has strong pseudo-*I*222 symmetry (Farber et al., 1987). The deviation from true *I*222 symmetry is caused by a slight tilt of one of the molecular 2-folds from the crystallographic axis. The tilt has been determined to be only 2.4° in magnitude, but it has a significant effect on the diffraction pattern even at medium resolution. The initial 3-Å resolution structure (Farber et al., 1987) was solved by multiple isomorphous replacement in the pseudosymmetric space group *I*222, because instrumental limitations

Table 1: Diffraction Data and Refinement Statistics

data set	native	glucose	3-*O*-methylglucose
metal	Mg	Mg	Mg
resolution (Å)[a]	∞–1.81	∞–1.96	∞–2.19
no. of crystals	2	1	2
reflections			
total	243152	225346	417620
unique	56756	53132	42123
completeness (%)	75	89	98
R_{merge}[b] (%)	5.1	7.8	4.3
wavelength	Cu Kα	Cu Kα	Mo Kα
temperature (°C)	4	4	20
resolution range used in refinement (Å)	10–1.81	10–1.96	10–2.19
R-factor (%)	16.1	16.6	15.9
rms deviation			
bonds (Å)	0.014	0.014	0.013
angles (deg)	2.7	2.6	2.7
dihedrals (deg)	23	23	24
impropers (deg)	1.1	1.1	1.1
no. of protein atoms	6048	6048	6048
no. of water molecules	496	481	450
av *B*-factor (Å^2) of			
protein main chain	16	14	14
protein side chain	20	18	18
waters	32	30	30

[a] Data completeness in the highest resolution shell (0.2-Å thickness) was similar to that overall. [b] $R_{merge} = \sum_i\sum_j|I_{ij} - I_i|/\sum_i\sum_j I_{ij}$.

restricted us to measuring only the strong data. Although the electron density map was of sufficient quality to reveal the overall folding of the polypeptide chain and the location of the active site, it was not possible to refine the structure properly or to extend the resolution without measuring all of the non-body-centered reflections, even at low resolution.

Collection of these data was not possible on a single-counter diffractometer with a sealed tube source, but it was achieved with the use of several area detectors. As refinement proceeded, it became apparent that several segments of the original 3-Å resolution model were out of registration with the amino acid sequence, in part because of sequence errors. Comparison of the 3-Å model with high-resolution structures determined elsewhere (Collyer et al., 1990) was extremely valuable in correcting these problems. To facilitate the construction of a correct model, we used the method of molecular replacement to position the *Arthrobacter* xylose isomerase in the *S. olivochromogenes* unit cell, initially by direct comparison with the 3-Å model, and as a control by *de novo* solution of the rotation and translation functions. Molecular replacement provided a correctly registered model of *S. olivochromogenes* xylose isomerase, which refined readily in the true $P2_12_12$ space group.

During the rebuilding, it was noticed that the electron density of some side chains disagreed with that of the originally reported amino acid sequence (Farber et al., 1989). Those areas that showed ambiguity were resequenced by us (E. Gerhardt-Müller and A. G. Glasfeld, unpublished results), but as the C-terminal domain is extremely GC base rich, sequencing was not successful in this region. In the region that could not be resequenced, the electron density alone was used to assess the correct amino acid type; in total, 13 amino acids were changed, five of which were in the C-terminal domain. The corrected *S. olivochromogenes* sequence and its alignment against four different xylose isomerases from different strains are shown in Figure 1.

S. olivochromogenes xylose isomerase belongs to the α/β-barrel structural family of proteins with eight alternating β-strands and α-helices (Farber & Petsko, 1990). The secondary structure elements are listed on the ribbon diagram in Figure 2. The crystallographic asymmetric unit is a dimer (Figure 3), although in the crystal the dimers form tetramers of 222 symmetry with one 2-fold axis coincident with the crystallographic 2-fold in space group $P2_12_12$. Xylose isomerase has a 67 amino acid C-terminal looplike domain, whose function appears to be stabilization of the tetramer (see below). The active sites, one in each monomer, are at the carboxy-terminal mouth of the parallel β-barrel, which is the typical position for α/β-barrel type proteins. The active site of each monomer in the asymmetric unit dimer contains residues from the other monomer, one of which is conserved (Phe25).

Native Structure. The active site of xylose isomerase has two metals ligated by a total of seven amino acid side chains. These residues are conserved in all known xylose isomerases (Figure 1). One metal, Mg-1, has four carboxylate ligands, while the second, Mg-2, has three carboxylate ligands and one imidazole ligand. One carboxylate, Glu216, serves as a bridging ligand between the two metals. Table 2 shows a list of ligands and distances. Mg-1 has four ligands donated by the carboxylate of Glu180, Glu216, Asp244, and Asp286; the angles deviate significantly from any ideal geometry. Mg-2 is octahedrally coordinated, receiving a single ligand from Glu216 and Asp256, the ϵ-nitrogen of the imidazole of His219, a putative hydroxide ion, and two ligands from Glu254. The single nonprotein ligand was modeled as a hydroxide ion (OH-1700 in the first monomer and OH-1800 in the second) and not as a water molecule due to its metal–ligand distance of 1.9 Å (in contrast to the longer distance observed in the substrate-soaked structures; see below). While the ligating residues are congregated to form a highly charged region, within 5–8 Å lie a number of conserved hydrophobic residues, including Phe93, Trp15, Trp136, and Phe25′ (Phe25′ originates from the second monomer). This arrangement of residues at the active site, polar on one side and hydrophobic on the other, produces an environment of "high hydrophobic contrast" (Yamashita et al., 1990). Lysine 182 and histidine 53 are the two other conserved residues in the active-site region, and their proposed roles will be discussed later.

Structure with Glucose. To understand substrate binding we soaked a crystal in glucose and collected X-ray data. Xylose isomerase is a one substrate, one product enzyme, and therefore the species observed in the crystal structure when the substrate is soaked at concentrations greater than K_M will be those present in the active site at equilibrium. The equilibrium on the enzyme between glucose and fructose is not known, but in solution it is 55:45 (Bock et al., 1983). The linear forms of glucose and fructose are nearly identical in shape. The only difference lies in which carbon, C1 or C2, has sp^2 hybridization and which has sp^3; therefore, we cannot distinguish between them from the electron density map at 1.96-Å resolution. We interpret the electron density to be glucose, but it probably represents a mixture of substrate and product.

Substrate binding was interpreted from electron density maps using the coordinates of the native model as the source of phases. As there were no sugar molecules in that coordinate file, there would be no phase bias for their presence. The difference electron density maps, both $3F_{obs} - 2F_{calc}$ and $F_{obs} - F_{calc}$ (difference map), had density near the metal binding site, to which the linear form of glucose could easily be fit (Figure 4). A second feature of the active site in the enzyme–substrate complex is that the density for Mg-2 is not spherical, as in the structure without substrate, but has an elliptical

```
                                                                                  †
Strep     1   ..........  ..........  ..........  ..SYQPTPED  RFTFG...LW  15
Actin     1   ..........  ..........  ..........  .MSVQATRED  KFSFG...LW  16
Clost     1   MNKYFENVSK  IKYEGPKSNN  PYSFKFYNPE  EVIDGKTMEE  HLRFSIAYWH  50
Ecoli     1   MQAYFDQLDR  VRYEGSKSSN  PLAFRHYNPD  ELVLGKRMEE  HLRFAACYWH  50

                      †                                                   †
Strep    16   TVGWQGRDPF  GDAT..RPAL  DPVETVQR..  .........L  AELGAHGVTF  52
Actin    17   TVGWQARDAF  GDAT..RTAL  DPVEAVHK..  .........L  AEIGAYGITF  53
Clost    51   TFTADGTDQF  GKATMQRPWN  HYTDPMDIAK  ARVEAAFEFF  DKINAPYFCF  100
Ecoli    51   TFCWNGADMF  GVGAFNRPWQ  QPGEALALAK  RKADVAFEFF  HKLHVPFYCF  100

              ††      †                                          † †
Strep    53   HDDDLIPFGS  SDTER....E  SHIKRFRQAL  DATGMTVPMA  TTNLFTHPVF  98
Actin    54   HDDDLVPFGS  DAQTR....D  GIIAGFKKAL  DETGLIVPMV  TTNLFTHPVF  99
Clost   101   HDRDIAPEGD  TLRETNKNLD  TIVAMIKDYL  KTSKTKVLWG  TANLFSNPRF  150
Ecoli   101   HDVDVSPEGA  SLKEYINNFA  QMVDVLAGKQ  EESGVKLLWG  TANCFTNPRY  150

                                                  † †        ††† †
Strep    99   KDGGFTANDR  DVRRYALRKT  IRNIDLAVEL  GAKTYVAWGG  REGAESGAAK  148
Actin   100   KDGGFTSNDR  SVRRYAIRKV  LRQMDLGAEL  GAKTLVLWGG  REGAEYDSAK  149
Clost   151   VHGASTSCNA  DVFAYSAAQV  KKALEITKEL  GGENYVFWGG  REGYETLLNT  200
Ecoli   151   GAGAATNPDP  EVFSWAATQV  VTAMEATHKL  GGENYVLWGG  REGYETLLNT  200
                                                      *
                                                  ††††  ††
Strep   149   DVRVALDRMK  EAFDLLGEYV  TSQGYDTRFA  IEPKPNEPRG  DILLPTVGHA  198
Actin   150   DVSAALDRYR  EALNLLAQYS  EDRGYGLRFA  IEPKPNEPRG  DILLPTAGHA  199
Clost   201   DMEFELDNFA  RFLHMAVDYA  KEIGFEGQFL  IEPKPKEPTK  HQYDFDVANV  250
Ecoli   201   DLRQEREQLG  RFMQMVVEHK  HKIGFQGTLL  IEPKPQEPTK  HQYDYDAATV  250
                                  *   *                       *
                    †             † †   †         †           † †
Strep   199   LAFIERLERP  ELYGVNPEVG  HEQMAGLNFP  HGIAQALWAG  KLFHIDLN.G  247
Actin   200   IAFVQELERP  ELFGINPETG  HEQMSNLNFT  QGIAQALWHK  KLFHIDLN.G  248
Clost   251   LAFLRKYDLD  KYFKVNIEAN  HATLAFHDFQ  HELRYARING  VLGSIDANTG  300
Ecoli   251   YGFLKQFGLE  KEIKLNIEAN  HATLAGHSFH  HEIATAIALG  LFGSVDANRG  300
                    * *                                           *
                    † †                                 †         †   †
Strep   248   QSGIKYDQDL  RFGAGDLRAA  FWLVDLLESA  .....GYE.G  PRHFDFKPPR  291
Actin   249   QHGPKFDQDL  VFGHGDLLNA  FSLVDLLENG  PDGAPAYD.G  PRHFDYKPSR  297
Clost   301   DMLLGWDTD   QFPTDIRMTT  LAMYEVIKMG  .....GFDKG  GLNFDAKVRR  344
Ecoli   301   DAQLGWDTD.  QFPNSVEENA  LVMYEILKAG  .....GFTTG  GLNFDAKVRR  344

Strep   292   TE DIDGVWA  SAAGCMRNYL  ILKERAAAFR  ADPEVQEALR  ...ASRLDEL  337
Actin   298   TE.DYDGVWE  SAKANIRMYL  LLKERAKAFR  ADPEVQEALA  ...ASKVAEL  343
Clost   345   ASFEPEDLFL  GHIAGMDAFA  KGFKVAYKLV  KDRVFDKFIE  ERYASYKDGI  388
Ecoli   345   QSTDKYDLFY  GHIGAMDTMA  LALKIAARMI  EDGELDKRIA  QRYSGWNSEL  388

Strep   338   AQPT..AADG  VQELLADRTA  FEDFDVDAAA  ARGMAFERLD  QLAMDHLLGA  385
Actin   344   KTPTLNPGEG  YAELLADRSA  FEDYDADAVG  AK.GFGFVKL  NQLAIEHLLG  391
Clost   389   GADIVSGKAD  FRSL..EKYA  LER...SQIV  NKSGRQ.ELL  ESILNQYLFA  436
Ecoli   389   GQQILKGQMS  LADL..AKYA  QEH.HLSP.V  HQSGRQ.EQL  ENLVNHYLFD  437

Strep   386   RG         387
Actin   392   AR.        394
Clost   437   E..        439
Ecoli   438   K..        440
```

FIGURE 1: Sequences of xylose isomerase compared from four different strains. The strains selected were those on which extensive site-directed mutagenesis was performed by various laboratories. Conserved residues in all 15 sequenced xylose isomerases are marked with a †. Those that participate in metal binding also have a * above the dagger. Abbreviations: Strep, *Streptomyces olivochromogenes*; Actin, *Actinoplanes missouriensis*; Clost, *Clostridium thermosulfurogenes*; Ecoli, *Escherichia coli*.

shape. We interpret this elliptical density as a shift of Mg-2 upon substrate binding from one site, called position 1 (the site occupied in the native structure), to a site closer to Mg-1 and the sugar, position 2. The distance between position 1 and position 2 is 1.8 Å. The sugar provides two full ligands to Mg-1 through O2 and O4. This changes the coordination of Mg-1, as compared to that in the native form, from tetracoordinate to octahedral (Table 2). The sugar makes further interactions with Mg-2 at position 2 by ligating through O1 and O2. When the sugar binds and Mg-2 is at position 2, its O2 becomes a bridging ligand between Mg-1 and Mg-2. O1 is also within hydrogen-bond distance of the ϵ-nitrogen of Lys182, which has been proposed to participate in the ring-opening reaction (Lambeir et al., 1992). The sugar is hydrogen-bonded further through O5 to the ϵ-nitrogen of His53. The water ligand (H_2O1700 in monomer 1 or 1800

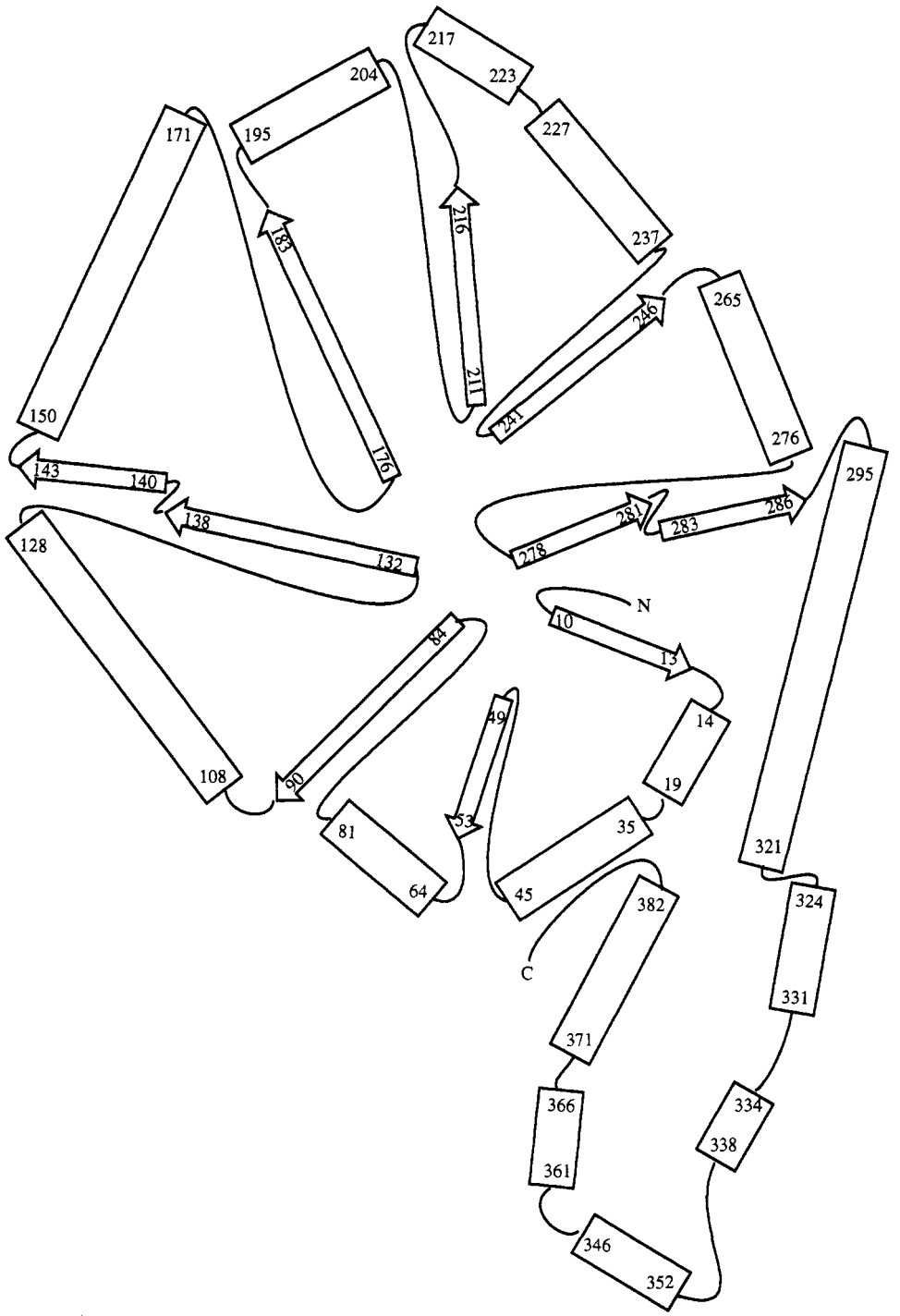

FIGURE 2: Secondary structure of xylose isomerase. Strands are depicted as arrows and α-helices as rectangles. The representation has the correct length proportions between α-helices and strands, based on 1.5 Å per residue in an α-helix and 3.5 Å per residue in a β-strand.

in monomer 2) of Mg-2 is seen clearly in the electron density. As the H_2O–Mg distance is 2.4 Å, we have modeled this ligand as water rather than as hydroxide ion, as it is in the native structure.

Structure with 3-O-Methylglucose. The electron density of the linear form of glucose can be difficult to distinguish from that of water molecules hydrogen-bonded in a series. Also, it is difficult to tell with a high degree of confidence in which direction to orient the glucose molecule. 3-*O*-Methylglucose was therefore utilized, as the position of the OCH_3 group should be unambiguous as a blob of electron density connected to O3. Since 3-*O*-methylglucose is a substrate for xylose isomerase, its mode of binding is expected to be the same as that of glucose. The relative positions of C1 and C6 of 3-*O*-methylglucose within the electron density are determined by the position of the OCH_3 group at C3; their orientation cannot be reversed. The kinetic parameters for 3-*O*-methylglucose versus those of glucose show that K_M is not significantly affected by the presence of the methyl group, although 3-*O*-methylglucose is about 500 times slower than glucose as substrate. A data set in which crystals of xylose isomerase were soaked with 3-*O*-methylglucose was collected and the structure was refined. The $F_{obs} - F_{calc}$ difference electron density map clearly shows the orientation of 3-*O*-methylglucose. Figure 5 depicts the 3-*O*-methylglucose difference map superimposed on the refined glucose model from the native plus the glucose structure. 3-*O*-Methylglucose binds in the same manner as glucose, forming the same

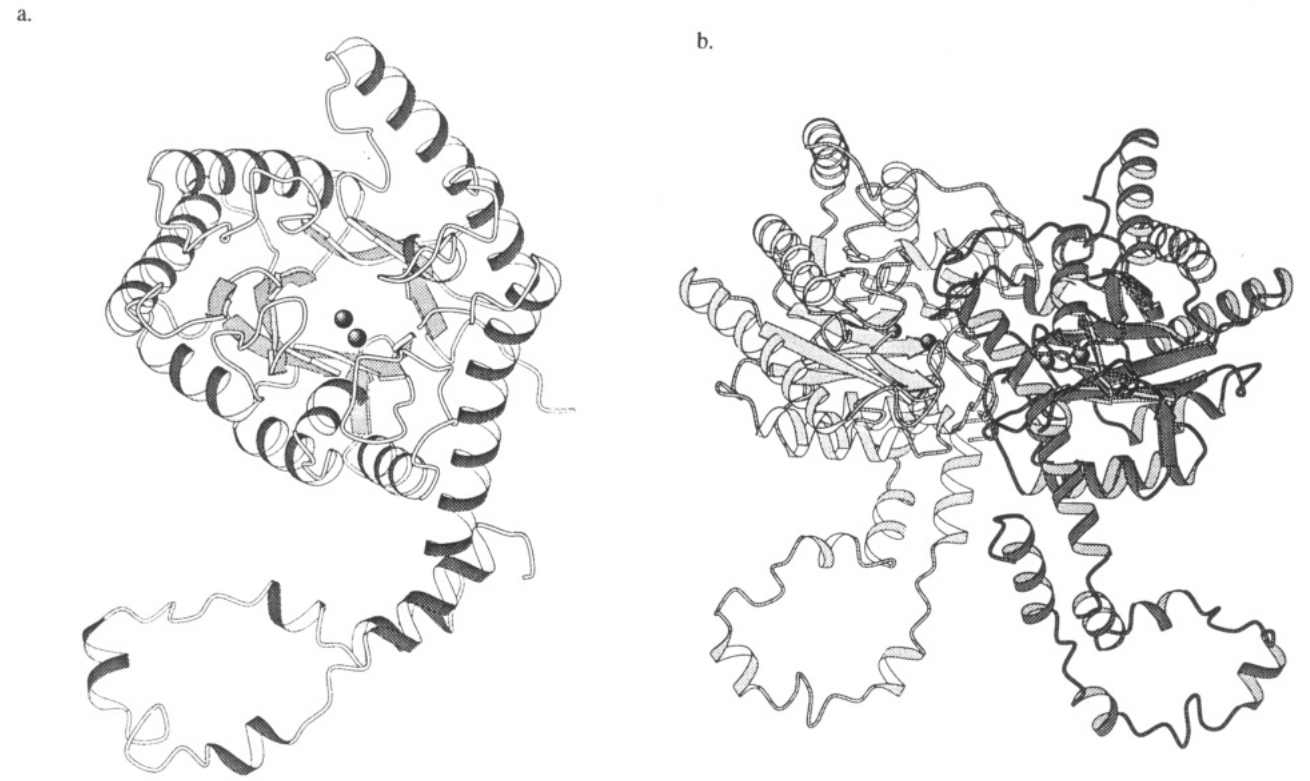

FIGURE 3: Monomer and the dimer in the asymmetric unit of xylose isomerase. (a) View down the barrel of a xylose isomerase monomer. The two metals are depicted as dark spheres. (b) The dimer in the asymmetric unit. This figure was rendered using the program Molscript (Kraulis, 1991).

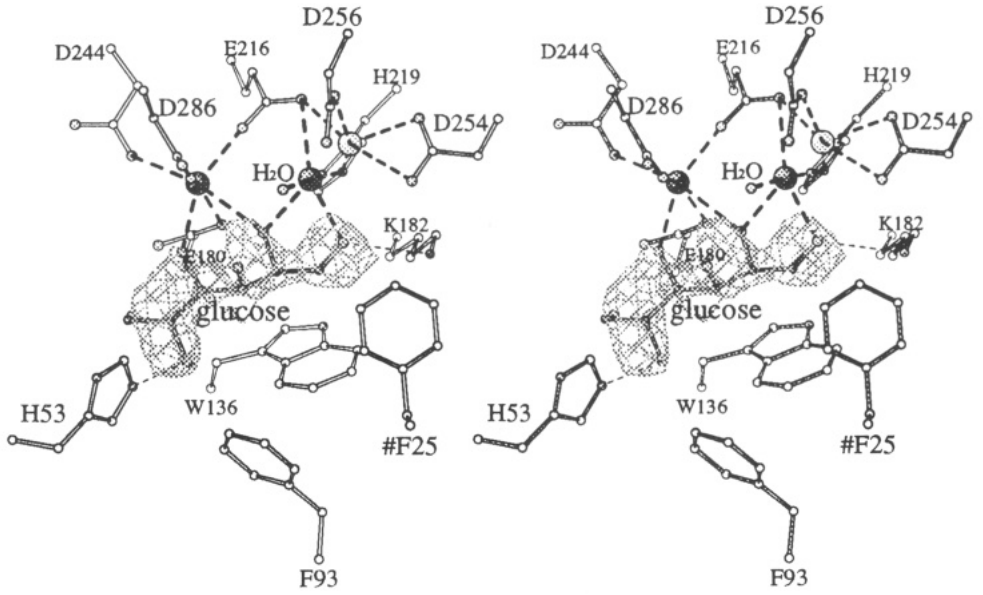

FIGURE 4: Stereodiagram showing the glucose molecule bound in the active site. The difference electron density, $F_{obs} - F_{calc}$, contoured at the 3σ level for the sugar, is also shown. Magnesium ions are depicted as large spheres; the dark spheres show Mg-1 and Mg-2 in position 2, and the light sphere shows Mg-2 in position 1. Position 2 of Mg-2 is only observed in the substrate-soaked structures. This figure was rendered using the program Molscript (Kraulis, 1991).

interactions with the magnesiums and protein residues His53 and Lys182 (Figure 4). As in the glucose-soaked structure, there are two positions for Mg-2, which is consistent with the interpretation that the presence of substrate is the cause for metal movement. The water ligand to Mg-2 is modeled as a water molecule and not as a hydroxide ion because the Mg-2–H_2O distance is 2.2 Å.

Solvent-Accessible Surface Area Calculations. Xylose isomerase is active as the tetramer (the crystals have isomerization activity) and possibly as the dimer (Callens et al., 1987). The tetramer (Figure 6c) can in theory be formed by three different combinations of dimers, where one is the dimer in the asymmetric unit (Figure 6b). The other two possible dimers (Figure 6d,e) were generated using the symmetry operators for $P2_12_12$, and the solvent-accessible surface area was calculated for all three dimers using the program Quanta (the probe size used was 1.4 Å). These were compared to the solvent-accessible area of the monomer (Figure 6a) to obtain an estimate of the area of interface for each dimer. This was done by multiplying the result from the solvent-accessible area calculation for the monomer by 2 (18 767 Å^2 × 2 = 37 544 Å^2) and subtracting each dimer

Table 2: Metal Ligands and Distances[a]

	structure								
	native			glucose			3-*O*-methylglucose		
		distance (Å)			distance (Å)			distance (Å)	
metal	ligand	Mon1	Mon2	liand	Mon1	Mon2	ligand	Mon1	Mon2
Mg-1	Glu180	2.7	2.1	Glu180	2.4	2.4	Glu180	2.5	2.5
	Glu216	2.2	2.6	Glu216	2.4	2.4	Glu216	2.3	2.4
	Asp244	2.4	2.6	Asp244	2.4	2.4	Asp244	2.5	2.5
	Asp286	2.2	2.6	Asp286	2.4	2.4	Asp286	2.4	2.5
				sugar O2	2.7	2.6	sugar O2	2.5	2.5
				sugar O4	2.5	2.5	sugar O4	2.7	2.5
Mg-2 position 1	Glu216	2.6	2.7	Glu216	2.5	2.5	Glu216	2.6	2.7
	His219	2.6	2.9	His219	2.9	2.7	His219	2.8	3.0
	Glu254	2.6	2.6	Glu254	2.4	2.4	Glu254	2.4	2.4
	Glu254	2.5	2.6	Glu254	2.5	2.5	Glu254	2.5	2.5
	Glu256	2.5	2.5	Glu256	2.4	2.4	Glu256	2.6	2.5
	H_2O	1.9	1.9	H_2O	*b*	*b*	H_2O	*b*	*b*
Mg-2 position 2	*c*			Glu216	2.7	2.6	Glu216	2.5	2.7
				His219	2.4	2.4	His219	2.4	2.6
				Glu254	(4.1)[a]	(4.0)	Glu254	(4.1)	(4.1)
				Glu254	(3.6)	(3.5)	Glu254	(3.6)	(3.7)
				Glu256	(3.7)	(3.4)	Glu256	(3.6)	(3.4)
				H_2O	2.4	2.4	H_2O	2.2	2.1
				sugar O1	2.3	2.4	sugar O1	2.5	2.6
				sugar O2	2.4	2.4	sugar O2	2.5	2.7

[a] Distances in parentheses are too long to be considered ligands. [b] This metal–water distance cannot be measured since the movement of Mg-2 results in an overlap of electron density with that of Mg-2 at position 2. [c] This site is only occupied in the presence of substrate.

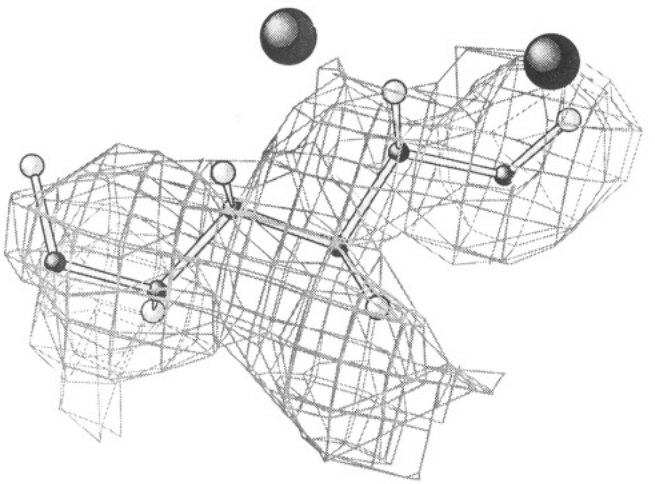

FIGURE 5: Difference Fourier electron density map ($F_{obs} - F_{calc}$) from the 3-*O*-methylglucose complex structure superimposed on the refined glucose model. The extra blob of density at O3 due to the methyl group is apparent. The metals are depicted as dark spheres. This figure was rendered using the program Molscript (Kraulis, 1991).

result from this number [for the asymmetric unit dimer (Figure 6b), 34 145 Å^2; for the "yin-yang" dimer (6d), 27 615 Å^2; for the "diagonal" dimer (6e) 34 310 Å^2]. The resultants [Figure 6b, 3389 Å^2; 6d, 9915 Å^2; and 6e, 3224 Å^2] are a good estimate for the area buried by the dimer interface. In order to determine the effect that the C-terminal tail of xylose isomerase has on the dimer interface area, the tail section (residues 320–386) was deleted from the models of each of the possible dimers. Solvent-accessible surface area calculations were carried out as before on the truncated dimers, and the dimer interface was computed from the results. The truncated dimer interface areas (3387, 3738, and 748 Å^2 for dimers in Figure 6b,d,e) show that the tail region does not contribute to the dimer interface of the asymmetric unit dimer (3389 Å^2 with tail, 3387 Å^2 without, Figure 6b), but almost triples that of the "yin-yang" dimer (9915 Å^2 with tail, 3738 Å^2 without, Figure 6d).

The interactions between the two monomers in the asymmetric unit dimer (Figure 6b) and in the "yin-yang" dimer (Figure 6d) were investigated further by counting the number of H-bonds and salt bridges between them. It was found that the asymmetric unit dimer had 1 H-bond and 4 bifurcated salt bridges between its two monomers, while the "yin-yang" dimer contained 40 H-bonds and 20 salt bridges (of which 12 are bifurcated) between its monomers.

DISCUSSION

We have attempted to understand the mechanism of glucose to fructose conversion by xylose isomerase. X-ray diffraction data from xylose isomerase crystals soaked with substrates were collected to obtain a detailed view of enzyme–substrate interactions. As the electron density of glucose or xylose can be fit in various ways due to their lack of distinguishing structural features, an experiment was designed to address that problem unambiguously. The crystallographic results using the substrate analog 3-*O*-methylglucose clearly demonstrate the mode of binding of this substrate to the enzyme. From this result, the mode of binding of glucose was established. On the basis of the work presented here and elsewhere (Allen et al., 1994a,b), and taking into consideration published results on xylose isomerase (Table 3), we can propose a mechanism that would be consistent with as much of the available data as possible (assuming an identical mechanism for xylose isomerases from various bacterial strains). This mechanism is outlined in Scheme 1. The unbound form of the enzyme is shown as compound I in Scheme 1.

Xylose Isomerase Active Sites from Different Sources. All recently published xylose isomerase structures contain two metals per subunit in the active site. Our native structure without substrate present shows that Mg-1 is tetracoordinate in agreement with Jenkins et al. (1992). However, Whitlow et al. (1991) and Carrel et al. (1989) observe an octahedral coordination of this metal; in addition to the four protein ligands to Mg-1, two water ligands were observed. This discrepancy can be explained by the presence of manganese cations in both of those structures instead of the magnesium in our

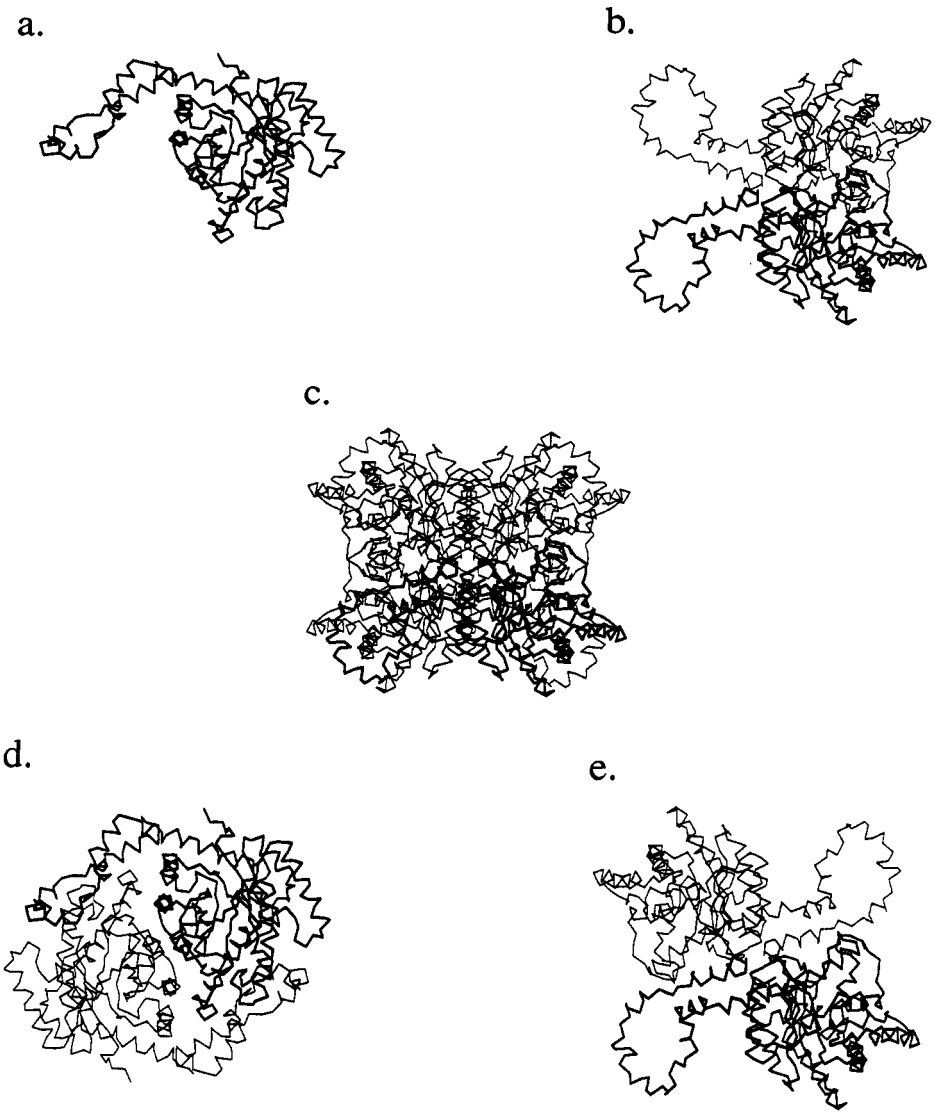

FIGURE 6: Cα tracings of a xylose isomerase: monomer (a), asymmetric unit dimer (b), tetramer (c) , and the two other possible dimers, the "yin-yang" dimer(d) and the "diagonal" dimer (e). This figure was rendered using the program Molscript (Kraulis, 1991).

structures. In the presence of substrate, Mg-1 is octahedrally ligated in all reported structures, utilizing O2 and O4 of the substrate in conjunction with the four protein ligands.

In all native structures Mg-2 is octahedrally coordinated with five protein ligands and one water molecule. In our native structure, the distance between Mg-2 and its water ligand is about 1.9 Å, which is more consistent with a Mg–hydroxide ligand distance (Bragg & Claringbull, 1965). In both of our substrate-soaked structures the metal–water distance is longer (~2.4 Å). Therefore, we propose that when no substrate is present this magnesium has a hydroxide ligand, which can accept a proton upon substrate binding or in a subsequent catalytic step. Two or more positions are assigned for Mg-2 by most groups (Jenkins et al., 1992; Whitlow et al., 1991), which implies metal movement during catalysis.

Proposed Mechanism. The first step of the reaction requires enzyme-catalyzed ring opening of the substrate since the noncatalyzed ring-opening reaction is slow compared to the rate of enzyme-catalyzed isomerization. The existence of catalysis of ring opening was questioned by the experimental evidence that no mutarotation activity was detected for xylose isomerase (Schray & Rose, 1971). To prove experimentally the existence of such a step, it was necessary to disconnect ring opening from isomerization. The xylose isomerase mutant E180K accomplishes this, since it catalyzes ring opening but lacks isomerization activity (Allen et al., 1994a). Ring opening can be catalyzed by either a base that will deprotonate O1 or by an acid that will protonate O5, the bridging ring oxygen. The search for the identity of the residues involved in ring opening has been only partially successful using X-ray crystallography. In all published structures of xylose isomerase with substrate present, the substrate is found in the open extended chain form, after ring opening has taken place.

Closed ring inhibitors were tried (Collyer & Blow, 1990; Collyer et al., 1992), with the resulting speculation that His53 is the ring-opening base. His53 has also been the favorite candidate for the ring-opening base by a number other groups (Carrel et al., 1989; Whitlow et al., 1991; Rangarjan & Hartley, 1992). This proposal, however, conflicts with the site-directed mutagenesis results; mutants lacking this histidine retain 4–16% isomerization activity and still catalyze ring opening (Lee et al., 1990; Lambeir et al., 1992; Gerhardt-Müller et al., unpublished results). The ring-closed α-anomer has been proposed to bind initially through O3 and O4 to Mg-1 (Rangarjan & Hartley, 1992; Collyer et al, 1990), thus orienting the bridging O5 near His53. The interaction of O3 with Mg-1 does not seem to be crucial, as demonstrated by the activity of substrates modified at the C3 position, like that of 3-*O*-methylglucose presented here or that of 3-deoxyglucose (Bock et al., 1983).

Table 3: Site-Directed Mutants of Xylose Isomerase

amino acid and sequence number in *S. olivochromogenes*	amino acid after mutation	activity	amino acid and sequence number in mutated strain	ref[g]
tryptophan 15	alanine	+,+	tryptophan 16,[a] tryptophan 49[b]	4, 10
	arginine	+	tryptophan 49[b]	10
	leucine	+	tryptophan 16[a]	4
	phenylalanine	+,+	tryptophan 16,[a] tryptophan 49[b]	4, 10
phenylalanine 25	histidine	+	phenylalanine 26[a]	4
	lysine	–		
proline 35	phenylalanine	+	histidine 71[c]	2
histidine 53	alanine	+,+	histidine 53,[d] histidine 54[a]	1, 4
	arginine	–	histidine 101[e]	9
	asparagine	+,+	histidine 101,[c] histidine 54[a]	2, 4
	aspartic acid	+	histidine 101[c]	2
	glutamic acid	+	histidine 101[c]	2
	glutamine	+,+	histidine 101,[c] histidine 54[a]	2, 4
	phenylalanine	–	histidine 101[c]	2
	tyrosine	–	histidine 101[c]	9
aspartic acid 56	asparagine	+	aspartic acid 57[a]	4
serine69/arginine 73[f]	serine/threonine	+	glycine 70/glycine 74[a]	6
serine 69/lysine 72/arginine 73[f]	serine/serine/threonine	+	glycine 70/alanine 73/glycine 74[a]	6
lysine 72[f]	serine	+	alanine 73[a]	6
methionine 87[f]	alanine	+	tryptophan 139[b]	10
	leucine	+		
	lysine	+		
	methionine	+		
	phenylalanine	+,+	tryptophan 139,[c] tryptophan 139[b]	8, 10
	tyrosine	+,+		
	valine	+	tryptophan 139[b]	10
methionine 87/valine 134[f]	phenylalanine/threonine	+	tryptophan 139/valine 186[c]	8
	phenylalanine/serine	+		
threonine 89[f]	serine	+	threonine 141[c]	8
aspartic acid 100	phenylalanine	+	histidine 152[c]	2
valine 134[f]	alanine	+	valine 186[c]	8
	serine	+		
	threonine	+		
tryptophan 136	glutamic acid	–	tryptophan 137[a]	4
	phenylalanine	+		
glutamic acid 180	alanine	–	glutamic acid 181[a]	3
	aspartic acid	+		
	glutamine	+		
	serine	–		
lysine 182	arginine	–	lysine 183[a]	4
	glutamine	–		
	serine	–		
glutamic acid 185	aspartic acid	+	glutamic acid 186[a]	5
	glutamine	+		
glutamic acid 216	aspartic acid	–	glutamic acid 217[a]	3
	glutamine	–		
	serine	+		
histidine 219	alanine	–	histidine 271[e]	9
	arginine	–		
	aspartic acid	–		
	asparagine	+,–	histidine 220,[a] histidine 271[e]	3, 9
	glutamine	+,–		
	leucine	–	histidine 271[e]	9
	lysine	–		
	phenylalanine	–		
	proline	–		
	serine	–		
	tyrosine	–		
aspartic acid 244	asparagine	–	aspartic acid 245[a]	3
lysine 252[f]	arginine	+	lysine 253[a]	6
	glutamine	+		
aspartic acid 254	alanine	–	aspartic acid 255[a]	3
	asparagine	+		
aspartic acid 256	asparagine	+	aspartic acid 257[a3]	3
	glutamic acid	+		
	lysine	–		
	serine	–		
aspartic acid 286	alanine	–	aspartic acid 292[a]	3
	asparagine	–		
	glutamic acid	–		
lysine 288	arginine	+,+	lysine 294[a]	4, 6
	asparagine	+		4
	glutamine	+		6
cysteine 305[f]	alanine	+	cysteine 305[d]	7

[a] *Actinoplanes missouriensis.* [b] *Thermoanaerobacterium thermosulfurigenes.* [c] *Clostridium thermosulfurogenes.* [d] *Streptomyces olivochromogenes.* [e] *Escherichia coli.* [f] Mutation was done to examine thermostability. [g] References: 1, Gerhardt-Müller (1993); 2, Lee et al. (1990); 3, Jenkins et al. (1992); 4, Lambeir et al. (1992); 5, Vantilbeurgh et al. (1992); 6, Quax et al. (1991); 7, Sicard et al. (1990); 8, Meng et al. (1991); 9, Batt et al. (1990); 10, Meng et al. (1993).

Scheme 1

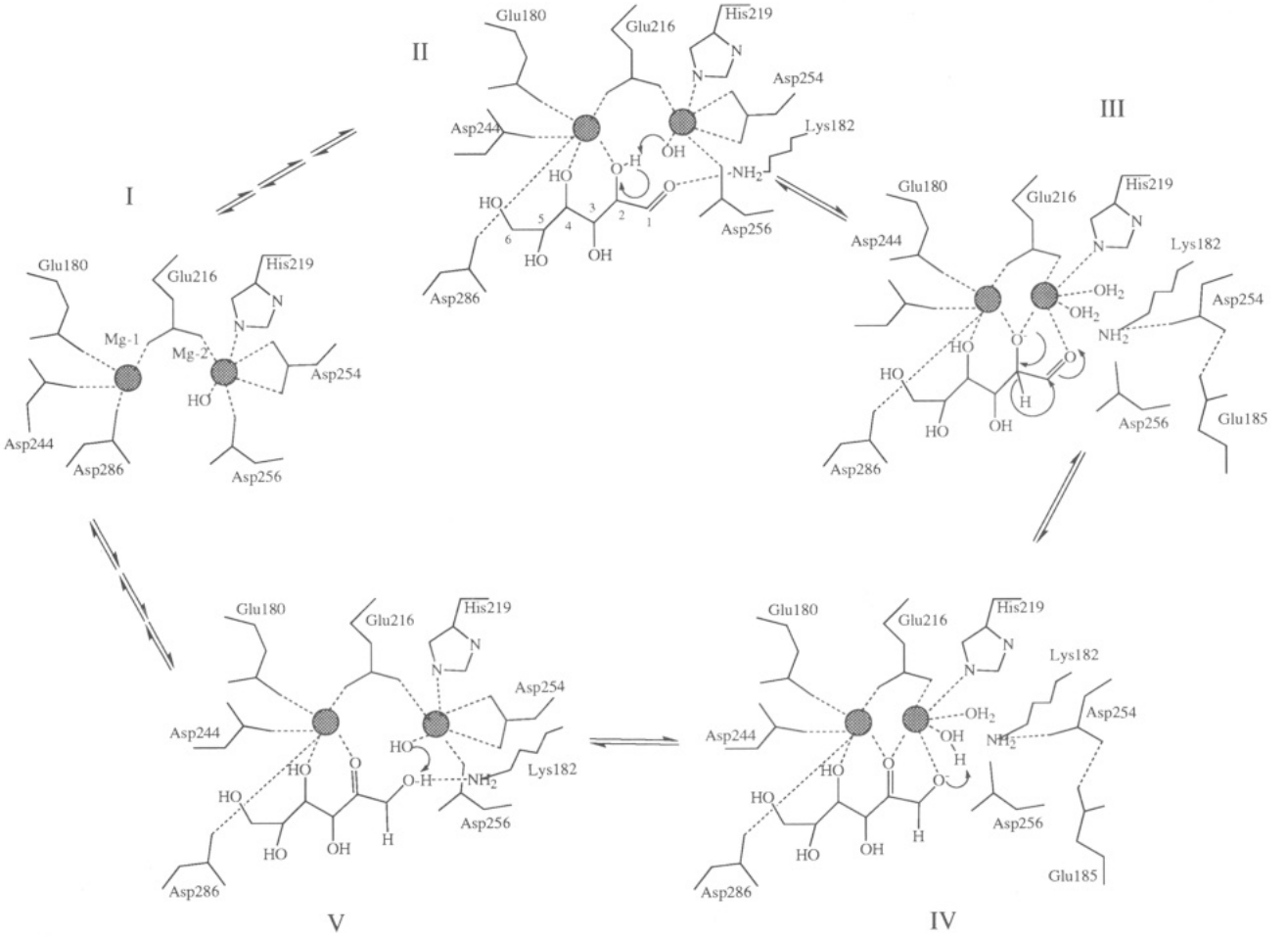

If His53 is not a ring-opening catalytic group, we can propose two possibilities for such a group. The first is Lys182, which is a conserved residue in all xylose isomerases and which makes a hydrogen bond to O1 of the linear sugar. Mutation of this residue to arginine, glutamine, or serine completely abolishes the activity (Table 3). Alternatively, the base can be the magnesium-bound hydroxide ion (water 1700 or 1800). Our structures are consistent with this ligand being a hydroxide ion prior to substrate binding and a water ligand thereafter. However, a mutant of xylose isomerase (E180K; Allen et al., 1994a) that catalyzes ring opening (the linear form of glucose is observed in the crystal structure), but not isomerization, also has a hydroxide ion bound to Mg-2 in position 1 (Mg-2 occupies only position 1 in this mutant structure). This observation is consistent with the hydroxide ion participating as a base in a reaction following ring opening (see below). The identity of the ring-opening group remains a subject for further investigation.

Once ring opening occurs, the sugar binds in a linear extended form (Scheme 1, compound II). Binding occurs by the formation of two additional bonds to the tetracoordinate Mg-1 through O2 and O4, forming an octahedral geometry, and also by coordinating through O2 and O1 with Mg-2, which moves to position 2, as seen in all crystal structures with substrates. Concomitant with sugar binding, or in a two-step process, O2 becomes deprotonated, and it is this change that is responsible for the shift of Mg-2 from position 1 to position 2 (Scheme 1, compound III). An alternative role to ring opening for the Mg-2-bound hydroxide is to participate as the proton acceptor in this step (Scheme 1, compound II). O2 of the sugar becomes a bridging ligand between Mg-1 and Mg-2, as seen most clearly in the crystal structure with the transition-state analog D-threonohydroxamate (Allen et al., unpublished results). The sugar is also held in place via a hydrogen bond to His53 from O5, but this interaction is not essential for catalysis, as demonstrated by site-directed mutagenesis of this residue (Lee et al., 1990; Jenkins et al., 1992; Gerhardt-Müller et al., unpublished results).

As Mg-2 moves from position 1 to position 2 (Scheme 1, compound III), it loses three protein ligands (two from Asp254 and one from Asp256) while forming only two new ligands with the sugar. Thus, it seems as if, upon substrate binding, there is a net loss of one ligand by Mg-2. However, it is possible that a water molecule moves in to fill this missing coordination, as seen in the structure of xylose isomerase with threonohydroxamate (Allen et al., unpublished results). In that structure, Mg-2 occupies only position 2; it breaks its protein ligands to Asp254 and Asp256 and compensates by forming two ligands with the hydroxamate and an additional ligand with a water molecule. This water ligand is in addition to the already ligated H_2O1700 or -1800. This water would not be observed in the substrate structures, because its electron density would be obscured by the partially occupied Mg-2 at position 1. Asp254 in the hydroxamate structure compensates for loss of the metal by forming hydrogen bonds with Glu185 and Lys182. These new interactions are not observed in the enzyme–substrate complexes.

Isomerization can then proceed by a hydride shift promoted by electrophilic catalysis (Scheme 1, compound IV). The electrophilic catalysis is provided by both metal ions. The requirement for the presence of both metal ions is demonstrated by mutants that selectively displace one metal preferentially.

The E180K mutant displaces Mg-1, but maintains the Mg-2 binding site intact (Allen et al., 1994a). Lambeir et al. (1992) have reported a similar mutant for Mg-2, where aspartic acid 254 was mutated into a lysine. In both cases, only the desired metal was displaced but the enzyme lost all activity. It is noteworthy that, in the E180K case, ring-opening activity was not abolished, as demonstrated by a ring-opening assay and as seen in the E180K–glucose complex structure (Allen et al., 1994a). For the D254K mutant, the linear sugar was observed in the crystal structure, but the possibility of scavenging of the linear form by the enzyme cannot be ruled out, as no direct measurement of ring-opening activity was reported.

In the glucose to fructose direction (Scheme 1, compound III → IV), Mg-2 can polarize the carbonyl group at C1. Polarization will induce a partial positive charge on C1, thus facilitating the hydride shift from C1 to C2. Lysine 182 may also participate in this process by H-bonding its ϵ-nitrogen with O1. Both metals are needed to stabilize the negative charge on O2. This mechanism is similar to the well-studied Meerwein–Pondorff–Verley–Oppenauer hydride-transfer reaction (Kemp & Vellacio, 1980). In these reactions, a metal acts as a Lewis acid coordinating to a carbonyl oxygen, thus polarizing the C=O bond and creating a partial positive charge on the carbonyl carbon. In the glucose to fructose direction, Mg-1 and Lys182 may act as the Lewis acid, inducing this positive charge formation on C1, while both metals act to stabilize the negative charge on O2 (Scheme 1, compound III). Both magnesiums simultaneously act to lower the pK_a of the sugar O2, facilitating its deprotonation. The deprotonated hydroxyl pulls the magnesiums closer together and establishes the proper catalytic geometry for the hydride transfer.

In the reverse reaction, fructose to glucose (Scheme 1, compound IV → III), substrate activation would be accomplished by both metals interacting with the carbonyl oxygen O2 of fructose, acting as the Lewis acid. Mg-2 in conjunction with Lys182 stabilizes the negative charge on O1, which was deprotonated by the hydroxyl ligand of the metal (Scheme 1, compound V).

Active-Site Environment. It has been noted that metals prefer to bind in environments of high hydrophobic contrast (Yamashita et al., 1990), and this is also the case in xylose isomerase. Segregation of an active site into a highly polar region and a hydrophobic region has been postulated to enhance metal binding, and we surmise that it also plays a role in enhancing substrate binding in xylose isomerase. In the crystal structures of xylose isomerase with substrate bound, most of the oxygens of the sugar point toward the metals, thus creating a hydrophobic surface with the carbon backbone. That surface can interact with Trp136, Phe93, and Phe25′. The importance of this effect is demonstrated by mutagenesis experiments (Table 3) on Trp136 (Lambeir et al., 1992). A change of Trp136 to a nonpolar residue does not abolish activity, but a change to glutamic acid does. The importance of Phe25′ is also demonstrated by site-directed mutagenesis; a change to the polar residue lysine abolishes activity (Lambeir et al., 1992). The amphiphilic nature of the active site seems to play a vital role in catalysis.

Activity as Dimer or Tetramer. The asymmetric unit in our crystal form is a dimer that packs into a tetramer in the crystal. Assuming that a dimer is sufficient for catalytic activity (Callens et al., 1987), one can ask which of the three possible dimers is the active solution dimer (Figure 6). The only dimer in which a crucial hydrophobic residue (Phe25′) completes the hydrophobic region is the dimer in the asymmetric unit (Figure 6b). This conclusion apparently contradicts the results of the solvent-accessible area calculations, which found the "yin-yang" dimer (Figure 6d) to possess a dimer interface 3 times greater in surface area than the asymmetric unit dimer or the other possible dimer (Figure 6b,e). It seems plausible that xylose isomerase, upon an increase in concentration, first aggregates into the "yin-yang" dimer, which is only slightly, or not at all, active. Only when this dimer forms the tetramer (dimer of dimers) does xylose isomerase become fully active. This result may establish a role for the C-terminal tail of xylose isomerase (Figure 2). Experiments that delete or alter the amino acid composition of this region abolish activity (G. Tiraby, unpublished results). Solvent-accessible surface area calculations show that the tail section accounts for two-thirds of the total dimer interface area of the "yin-yang" dimer, but makes no contribution to the dimer in the asymmetric unit. A function for this region may lie in its ability to force dimerization, albeit into an inactive dimer. This dimer can then associate into the tetramer, resulting in the fully functional enzyme.

ACKNOWLEDGMENT

We thank Prof. Emil Pai (University of Toronto) for collecting the data on the glucose-soaked crystal at the Max Planck Institute in Heidelberg, FRG, and Dr. Keith Wilson and Dr. Zbigniew Dauter for help in collecting the 3-*O*-methylglucose data set at the EMBL in Hamburg, FRG. We are grateful to Dr. Charles Collyer and Prof. David Blow for discussions that facilitated our progress to a high-resolution structure. We thank Dr. James Clifton for a program that analyzes interresidue interactions. We are grateful to Drs. Gregory Farber, Arthur Glasfeld, and Eva Gerhardt-Müller for useful discussions. Special thanks are due to Dr. Ilme Schlichting and Dr. Shigetoshi Sugio for their valuable help and suggestions throughout this project.

REFERENCES

Albery, W. J., & Knowles, J. R. (1976) *Biochemistry 15*, 5627–5631.

Allen, K. N., Lavie, A., Glasfeld, A., Tanada, T. N., Gerrity, D. P., Carlson, S. C., Farber, G. K., Petsko, G. A., & Ringe, D. (1994a) *Biochemistry 33*, 1488–1494.

Allen, K. N., Lavie, A., Farber, G. K., Glasfeld, A., Petsko, G. A., & Ringe, D. (1994b) *Biochemistry 33*, 1481–1487.

Batt, C. A., Jamieson, A. C., & Vandeyar, M. A. (1990) *Proc. Natl. Acad. Sci. U.S.A. 87*, 618–22.

Blacklow, S. C., Raines, R. T., Lim, W. A., Zamore, P. D., & Knowles, J. R., (1988) *Biochemistry 27*, 1158–1167.

Bock, K., Meldal, M., Meyer, B., & Wiebe, L. (1983) *Acta Chem. Scand. B37*, 101–108.

Bragg, L., & Claringbull, G. F. (1965) in *The Crystalline State—Vol. IV: Crystal Structures of Minerals* (Bragg, L., Ed) pp 116–119, G. Bell & Sons Ltd., London.

Brünger, A. T. (1992) in *X-PLOR (Version 3.0) Manual*, Yale University, New Haven, CT.

Callens, M., Vangrysperre, W., Kersters-Hilderson, H., & De Bruyne, C. K. (1987) *Arch. Int. Physiol. Biochim. 95*, B64.

Carrell, H. L., Rubins, B. H., Hurley, T. J., & Glusker, J. P. (1984) *J. Biol. Chem. 259*, 3230–3236.

Carrell, H. L., Glusker, J. P., Burger, V., Manfre, F., Tritsch, D., & Biellmann, J.-F. (1989) *Proc. Natl. Acad. Sci. U.S.A. 86*, 4440–4444.

Collyer, C. A., & Blow, D. M. (1990) *Proc. Natl. Acad. Sci. U.S.A. 87*, 1362–1366.

Collyer, C. A., Henrick, K., & Blow, D. M. (1990) *J. Mol. Biol. 212*, 211–235.

Collyer, C. A., Goldberg, J. D., Viehmann, H., Blow, D. M., Ramsden, N. G., Fleet, G. W. J., Montgomery, F. J., & Grice, P. (1992) *Biochemistry 31*, 12211–12218.
Crowther, R. A., & Blow, D. M. (1967) *Acta Crystallogr. 23*, 544–548.
Dauter, Z., Terry, H., Witzel, H., & Wilson, K. S. (1990) *Acta Crystallogr. B46*, 833–841.
Farber, G. K., Petsko, G. A. (1990) *Trends Biochem. Sci. 15*, 228–234.
Farber, G. K., Petsko, G. A., & Ringe, D. (1987) *Protein Eng. 1*, 459–466.
Farber, G. K., Glasfeld, A., Tiraby, G., Ringe, D., & Petsko, G. A. (1989) *Biochemistry 28*, 7289–7297.
Gerhardt-Müller, E. (1993) Ph.D. Thesis, Heidelberg University, Heidelberg, FRG.
Henrick, K., Collyer, C. A., & Blow, D. M. (1989) *J. Mol. Biol. 208*, 129–157.
Hodel, A., Kim, S.-H., & Brünger, A. T. (1992) *Acta Crystallogr. A48*, 851–858.
Jenkins, J., Janin, J., Rey, F., Chiadmi, M., van Tilbeurgh, H., Lasters, I., De Maeyer, M., Van Belle, D., Wodak, S. J., Lauwereys, M., Stanssens, P., Mrabet, N. T., Snauwaert, J., Matthyssens, G., & Lambeir, A.-M. (1992) *Biochemistry 31*, 5449–5458.
Jones, T. A. (1978) *J. Appl. Crystallogr. 11*, 268–272.
Kabsch, W. (1988) *J. Appl. Crystallogr. 21*, 916–924.
Kemp, D. S., Vellaccio, F. (1980) in *Organic Chemistry*, Worth Publishers Inc., New York.
Kraulis, P. J. (1991) *J. Appl. Crystallogr. 24*, 946–950.
Lambeir, A.-M., Lauwereys, M., Stanssens, P., Mrabet, N. T., Snauwaert, J., van Tilbeurgh, H., Matthyssens, G., Lasters, I., De Maeyer, M., Wodak, S. J., Jenkins, J., Chiadmi, M., & Janin, J. (1992) *Biochemistry 31*, 5459–5466.
Lee, C., Bagdasarian, M., Meng, M., & Zeikus, G. (1990) *J. Biol. Chem. 265*, 19082–19090.
Meng, M., Lee, C., Bagdasarian, M., & Zeikus, G. (1991) *Proc. Natl. Acad. Sci. U.S.A. 88*, 4015–4019.
Meng, M., Bagdasarian, M., & Zeikus, J. G. (1993) *Proc. Natl. Acad. Sci. U.S.A. 90*, 8459–63.
Quax, W. J., Mrabet, N. T., Luiten, R., Schuurhuizen, P. W., Stanssens, P., & Lasters, I. (1991) *BioTechnology 9*, 738–742.
Rangarajan, M., & Hartley, B. S. (1992) *Biochem. J. 283*, 223–233.
Rao, S. N., Jih, J.-H., & Hartsuck, J. A. (1980) *Acta Crystallogr. A36*, 878–884.
Reider, S. V., & Rose, I. A. (1959) *J. Biol. Chem. 234*, 1007–1010.
Rey, F., Jenkins, J., Janin, J., Lasters, I., Alard, P., Claessens, M., Matthyssens, G., & Wodak, S. (1988) *Proteins: Struct., Funct., Genet. 4*, 165–172.
Rossmann, M. G., & Blow, D. M. (1962) *Acta Crystallogr. 15*, 24–31.
Schray, K. J., & Rose, I. A. (1971) *Biochemistry 10*, 1058–1062.
Sicard, P. J., Leleu, J.-B., Duflot, P., Drocourt, D., Martin, F., Tiraby, G., Petsko, G., & Galsfeld, A. (1990) *Ann. N.Y. Acad. Sci. 613*, 371–373.
van Tilbeurgh, H., Jenkins, J., Chiadmi, M., Janin, J., Wodak, S. J., Mrabet, N. T., & Lambeir, A.-M. (1992) *Biochemistry 31*, 5467–5471.
Whitlow, M., Howard, A. J., Finzel, B. C., Poulos, T. L., Winborne, E., & Gilliland, G. L. (1991) *Proteins: Struct., Funct., Genet. 9*, 153–173.
Yamashita, M. M., Wesson, L., Eisenman, G., & Eisenberg, D. (1990) *Proc. Natl. Acad. Sci. U.S A. 87*, 5648–5652.